15

AC/AC Converters

Mehrdad Kazerani
University of Waterloo, Waterloo, Ontario, Canada

15.1 INTRODUCTION

In this chapter, AC/AC converter refers to a static frequency changer mainly made up of semiconductor switches, which is used to convert the AC power at a given frequency to the AC power at a desired frequency.

AC-to-AC conversion can be indirect or direct depending on whether or not the process includes an intermediate DC stage (DC link). Frequency conversion can be restricted or unrestricted, depending on whether or not the achievable output frequency range is limited by the input frequency. Depending on the application, an AC/AC converter can accommodate conversion from a variable frequency to a fixed frequency or vice versa.

Since the introduction of the first mercury-arc static frequency changer prototype in the early 1930s [1], the advances in semiconductor technology, power electronics, and control theory have resulted in a huge progress in the performance and applications of AC/AC converters. Static frequency changers find applications in AC motor drives and, thus, in the automotive industry, which is moving towards more electric vehicles (MEVs). With an internal combustion engine (ICE) driving a synchronous or induction generator, the AC/AC converter can convert the AC power produced to variable frequency AC power, which will be used to drive the motor engaged with the wheels at the desired speed.

The following sections introduce different established AC/AC converter topologies together with their advantages, disadvantages, and restrictions. The objective of this chapter is to familiarize the reader with the established AC/AC converter topologies and their potentials in the automotive industry, especially with regard to hybrid electric vehicles (HEVs). The references cited in this chapter provide sources of detailed information for further study.

15.2 AC/AC CONVERTER TOPOLOGIES

AC/AC converter topologies fall under two major categories, indirect and direct. In the following sections, these topologies will be described.

15.2.1 INDIRECT AC/AC CONVERTER

Indirect or DC-link AC/AC converters are composed of two back-to-back voltage- or current-source converters, connected via a DC-link capacitor or reactor. Figure 15.1 and Figure 15.2 show the schematic diagrams of the voltage- and current-source converter-based indirect AC/AC converters. The switches S_{a+}, S_{b+}, …, S_{C-} in Figure 15.1 and Figure 15.2 are unidirectional switches, respectively.

The indirect AC/AC converter topology has also been called rectifier-inverter pair. Depending on the mode of operation being "motoring" or "regenerative breaking," one of the two back-to-back converters assumes the role of a "rectifier," and the other converter will act as an "inverter." The two converters in each topology can be controlled using phase-control, pulse-width modulation (PWM), space vector modulation (SVM), or selective harmonic elimination (SHE) technique. The DC terms, V_d and I_d, in voltage- and current-source converter-based topologies, respectively, are regulated by closed-loop control systems to ensure input/output real power balance.

The advantages of the indirect AC/AC converter topology lie in its low number of components, its simplicity of control, the possibility of simultaneous input power factor control and output vector control, the ride-through capability due to the existence of a DC-link energy storage element, and the immunity to the adverse effects of harmonic distortion and imbalance in the input voltage.

The disadvantages of the indirect AC/AC converter topology lie in the presence of the DC-link reactive elements that add to the weight, size, and cost of the scheme, and

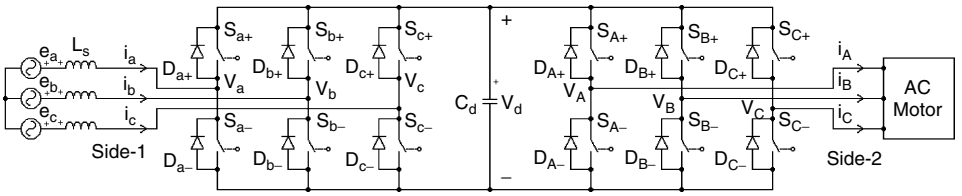

Figure 15.1 Voltage-source converter-based indirect AC/AC converter.

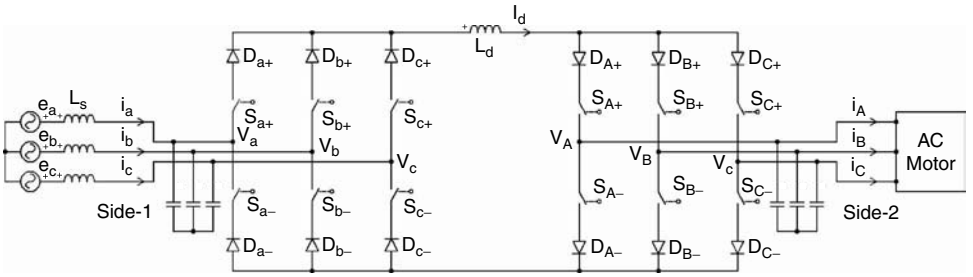

Figure 15.2 Current-source converter-based indirect AC/AC converter.

the fact that a high DC-link voltage ($V_d > 1.634\ V_{LL}$ for two-level PWM voltage-source converter-based topology) or current ($I_d > 1.616\ I$ for three-level PWM current-source converter-based topology) has to be maintained in order to be able to produce the required output AC voltage and current over the entire operating range, thus adding to the losses and device ratings. If the instantaneous input/output power balance is maintained through implementation of a proper control strategy, the need for energy storage in the DC-link can be dramatically reduced, leading to a quasi-direct AC/AC converter [2]. Also, if the DC-link current in the current-source converter-based topology is adjusted based on the load requirements, the losses due to high DC-link currents can be minimized.

Current-source converter-based AC/AC converters are used for medium- to high-power motor drives, especially if a long cable is needed between the converter and the motor in applications such as submerged pumps. In this situation, a voltage-source converter-based AC/AC converter is not appropriate, as the output pulsed-voltage traveling wave can result in destructive overvoltages at the motor terminals. This can damage the insulation of the motor windings in the first few turns unless specially designed motors, which are more expensive than the ordinary ones, are used. Voltage-source converter-based AC/AC converters are more commonly used as AC motor drives and are more likely to be used in hybrid electric vehicles due to their higher efficiency and possibility of using a battery directly across the DC link for energy storage. The lower efficiency of current-source converter-based topology is attributed to the higher conduction losses in this topology due to the presence of diodes, which are placed in series with the switches to enhance the reverse voltage withstand capability, as well as the fact that the DC-link inductors are more lossy than the DC-link capacitors. Figure 15.3 and Figure 15.4 show the block diagrams of the HEV series and parallel designs that can be realized by the voltage-source converter-based AC/AC converter topology.

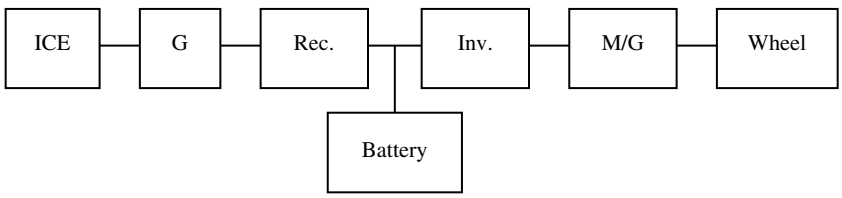

Figure 15.3 HEV serial design based on voltage-source converter-based AC/AC converter.

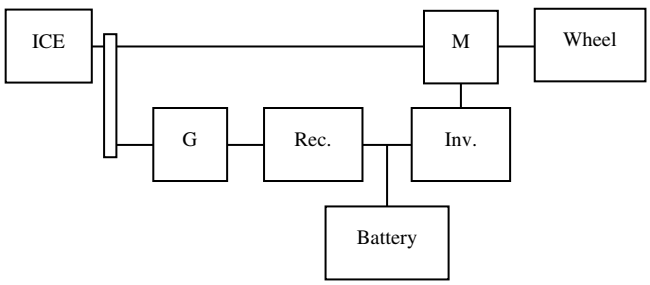

Figure 15.4 HEV parallel design based on voltage-source converter-based AC/AC converter.

Indirect AC/AC converter is an unrestricted frequency changer, as the output frequency is independent of the input frequency. When operating at a moderately high switching frequency, the qualities of the input and output waveforms are very high, with no low-order harmonics and, thus, minimal filtering requirements. Also, the dynamic response will be faster due to higher control bandwidth. In order to enjoy the benefits of high switching frequency while avoiding high switching losses and electromagnetic interference (EMI), soft-switched high-frequency converters have been proposed based on parallel resonant DC-link (RDCL) and series RDCL [3]. Even though the resonant topologies feature better performance and higher power density, they are not as established as the original hard-switched voltage- and current-source converter-based topologies and are known to have lower reliability and higher cost [3].

15.2.2 Direct AC/AC Converter

In direct AC/AC converter topology, the DC-link reactive element is eliminated, allowing for a more compact design. However, the number of components will be higher compared with that of the rectifier-inverter pair. Furthermore, the system lacks ride-through capability.

Direct AC/AC converters are divided into two major categories, naturally and forced-commutated cycloconverters.

15.2.2.1 Naturally Commutated Cycloconverter (NCC)

Figure 15.5 shows the schematic diagram of a three-phase-to-three-phase NCC. NCCs are based on the mature technology of SCRs (thyristors) and are operated under phase-control technique. NCCs are considered to be more efficient, less costly, and lighter than the rectifier-inverter pair AC/AC converters [4]. The high-power handling capability of SCRs makes the NCC the natural choice for high-power frequency changers. The operational limitation of NCC is in the output frequency. In order for the variation of the firing angles of the SCRs in the NCC to follow the typical sequence of commutation between the successive phases, the output frequency has to be lower than or equal to one third of the input frequency, making NCC a restricted frequency changer. This limitation will not be an issue when the input-to-output frequency ratio is high, as is the case when AC power is generated by high-speed generators. This high frequency ratio results in very high-quality output waveforms, as well as very fast dynamic response. On the other hand, operating at high input frequency asks for high-speed SCRs, which are more expensive. The other advantage of NCC is in the inherent zero-current switching (ZCS) capability of SCRs, resulting in low switching losses. In contrast to NCC, a hard-switched rectifier-inverter pair suffers high switching losses.

NCC is based on the dual converter topology and may be operated under circulating-current or noncirculating-current control. Figure 15.6(a) and Figure 15.6(b) show the schematic diagrams of one phase of the circulating current and noncirculating current NCC topologies, respectively. In the circulating current NCC, both P and N converters are operated simultaneously, where the firing angles of the thyristors in the two converters are related through $\alpha_N = 180^\circ - \alpha_P$. As in this case, the instantaneous DC-side voltages of the two converters are different, even though the average values are the same, inductors are used on the DC side between the two converters to make the connection of two unequal voltages possible and limit the circulating current. In the noncirculating current NCC, the P converter is operated at the firing angle α when the load current is positive, whereas the N converter is operated at the firing angle $\alpha_N = 180^\circ - \alpha_P$ when the load current is negative. The noncirculating-current NCC, which has been referred to as the practical

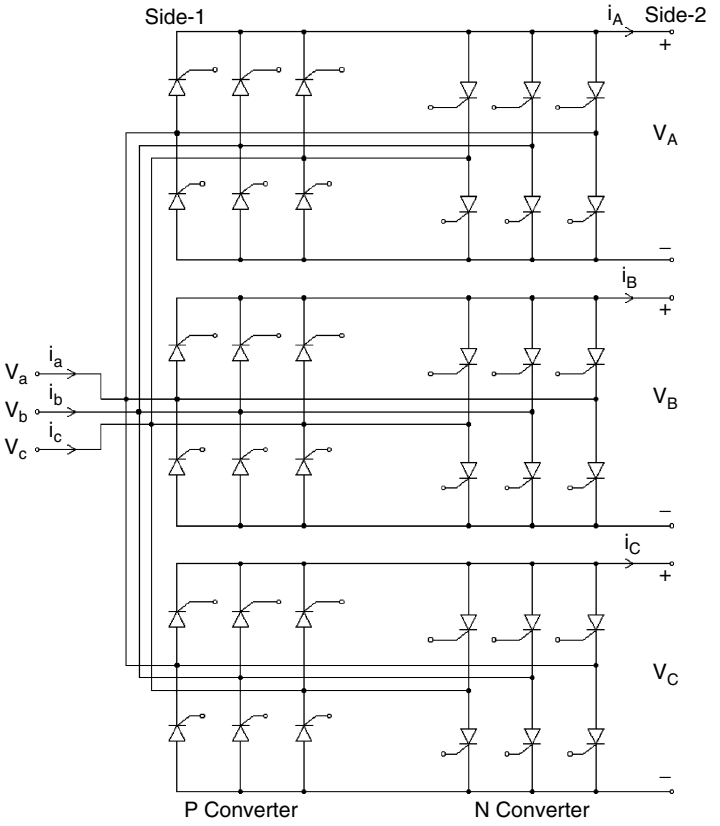

Figure 15.5 Schematic diagram of a three-phase NCC.

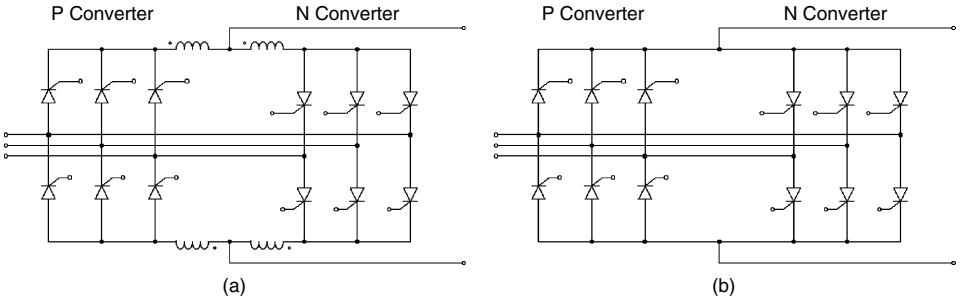

Figure 15.6 (a) Circulating current NCC; (b) noncirculating current NCC.

cycloconverter [5], due to its higher efficiency and more compact design, is potentially more feasible in hybrid electric vehicles. The control of the firing angles of the SCRs in the dual converters is based on the cosine-wave intersection method [6,7]. In this method, a sinusoidal modulating signal of amplitude between 0 and 1 at the desired output frequency is intersected with a timing cosine waveform of amplitude 1 at the input frequency. The firing angle α is then calculated as the angle corresponding to the points of intersection of the modulating signal with the falling edges of the timing signal in different cycles

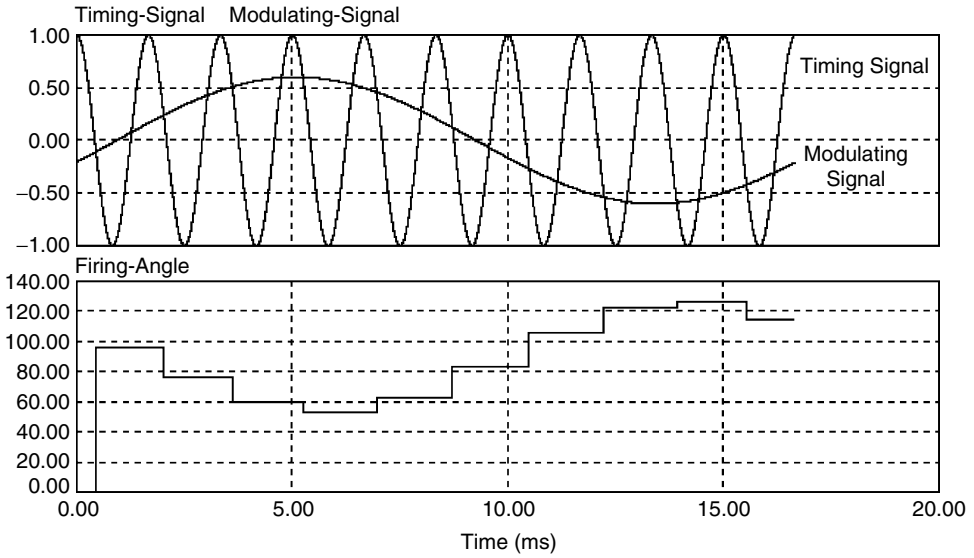

Figure 15.7 Cosine-wave intersection method.

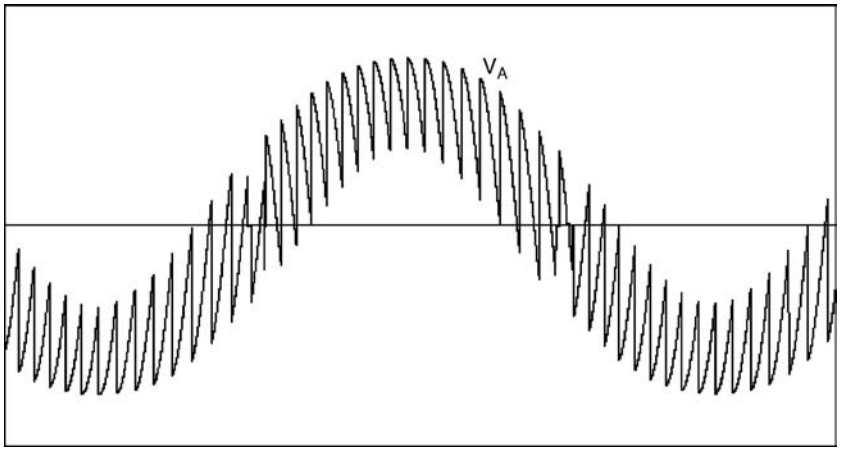

Figure 15.8 Typical output voltage waveform of NCC.

(Figure 15.7). The firing angle is updated once in every cycle of the input signal. This means that in NCC, the control bandwidth is limited by the input frequency. The local average of the output voltage of the noncirculating current NCC is given by 1.35 V_{LL} cos α_P [6], where V_{LL} is the rms value of the line-to-line input voltage and α_P is the firing angle of the P converter valves. In order to realize the desired output voltage, a modulating signal of the form $v_m = M \cos(\omega t + \theta)$ is produced by a closed-loop control circuit, where $0 \leq M \leq 1$, ω is the angular frequency of the output voltage, and θ is the desired phase angle of the output voltage. This signal is input to a $\cos^{-1}$ block whose output is used as the firing angle for the converter valves. As a result, the local average of the output voltage of the dual converter becomes 1.35 V_{LL} Mcos $(\omega t + \theta)$, implying that in local average sense, the dual converter behaves as a linear amplifier that duplicates the modulating signal

at its output terminals with a gain of 1.35 V_{LL}. Figure 15.8 shows a typical output voltage waveform for one output phase of NCC (v_A in Figure 15.5). The fundamental component of the output voltage waveform is clearly seen as the center-line, with high-frequency components making a band around it.

When operating under noncirculating-current control, either the three-phase voltages feeding the dual converters or the output phases have to be isolated from one another to avoid interaction between the dual converters [6]. To avoid isolation transformers and reduce the size and weight of the system, the high-speed generator or the traction motor has to have isolated three-phase windings.

A major disadvantage for NCC is its low and uncontrollable input displacement power factor due to the fact that phase-controlled thyristor converters draw reactive power from the source irrespective of the mode of operation (rectifier or inverter). The need for additional devices for input reactive power compensation and power factor correction makes NCC a poor choice for the hybrid electric vehicle industry. Another major disadvantage for NCC is the low-order harmonic distortion of the input current. Addition of harmonic filters to eliminate harmonics makes the scheme more costly and less competitive.

15.2.2.2 Forced-Commutated Cycloconverter (Matrix Converter)

The conventional three-phase forced-commutated cycloconverter (FCC) or matrix converter is composed of an array of nine bidirectional switches, each connected between one phase of the input and one phase of the output. A matrix converter is an unrestricted frequency changer, which constructs the output voltage waveforms by piecing together selected segments of the input voltage waveforms [8]. Figure 15.9 shows the schematic diagram of a conventional matrix converter.

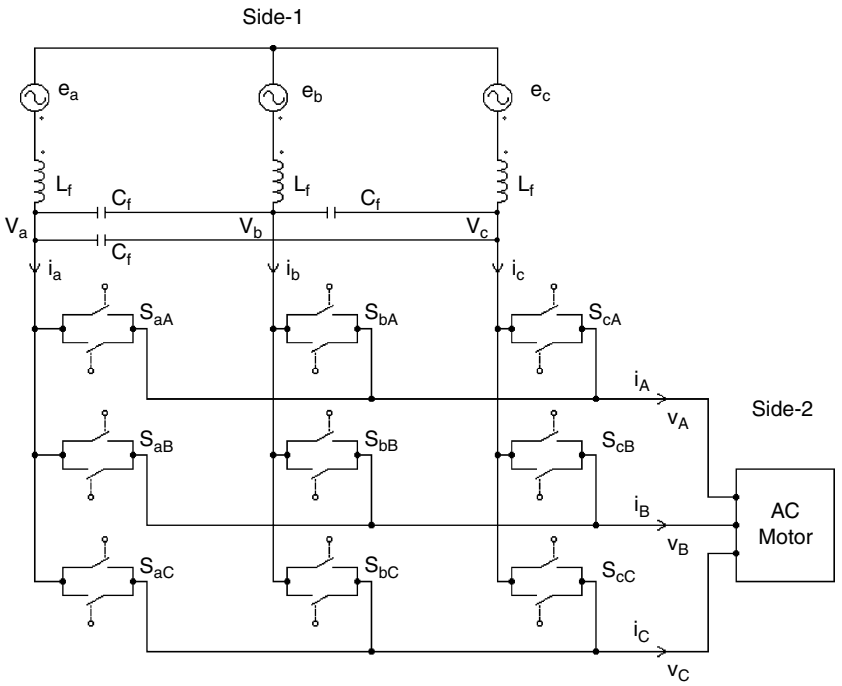

Figure 15.9 Schematic diagram of a conventional matrix converter.

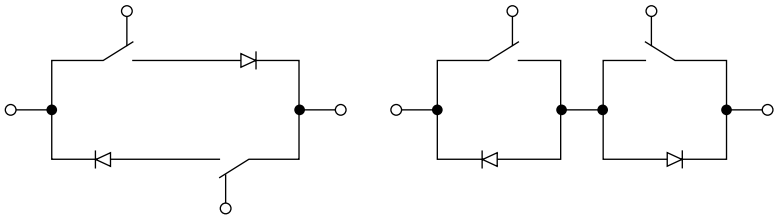

Figure 15.10 Two possible structures for bidirectional switch.

A bidirectional switch is composed of two two-quadrant switch elements connected in one of the two ways shown in Figure 15.10, which is capable of conducting current in both directions in the on-state and blocking voltages of both polarities in the off-state. For this reason, a bidirectional switch is commonly referred to as a four-quadrant switch. To date, no monolithic four-quadrant switch is available off the shelf.

The 9-bidirectional-switch matrix converter topology, when realized by any of the two bidirectional switch configurations of Figure 15.10, uses 18 unidirectional switches and 18 fast-recovery diodes. New advancements in the semiconductor technology have led to the introduction of forward and reverse blocking non-punch-through (NPT) IGBTs, eliminating the need for the diode that has to be placed in series with each unidirectional switch in Figure 15.10(a) when constructing a bidirectional switch [9]. Using the new bidirectional switch configuration based on the NPT IGBT switches reduces the number of semiconductor elements in the 9-bidirectional-switch matrix converter topology to 18 switches and 0 diodes. This brings the matrix converter in a real competitive position with respect to the well-known rectifier-inverter pair topology.

Note that voltage-source converter-based indirect AC/AC converter topology has 12 unidirectional switches, 12 fast-recovery diodes, and one DC-link capacitor. The current-source converter-based rectifier-inverter pair AC/AC converter uses 12 unidirectional switches, 12 fast-recovery diodes, and one DC-link inductor. In current-source converter-based topology, the number of semiconductor devices is reduced to 12 unidirectional switches and 0 diodes if NPT IGBTs are used. However, the need for the DC-link inductor will be a serious disadvantage for the current-source converter-based topology until superconductive materials for magnetic energy storage become affordable for public applications. Furthermore, a current-source converter-based AC/AC converter is not appropriate for hybrid electric cars, as direct integration of battery for energy storage on the DC-link is not possible. It is said that the success of the matrix converter topology depends on the availability of monolithic bidirectional switches to reduce the semiconductor component count [3].

Due to the special arrangement of the switches, at any moment of time, one and only one of the three switches connecting the three phases of the input to each phase of the output (e.g., S_{aA}, S_{bA}, and S_{cA} in Figure 15.9) has to be on, to avoid short-circuiting of the side-1 voltage sources or interrupting the side-2 inductive load currents. This constraint reduces the number of possible switch-state combinations from $2^9 = 512$ to 27 valid states [10]. From the practical point of view, translating the calculated switch duty ratios into actual gating signals requires distribution of the on-periods of the switches over each switching period according to a special pattern. This distribution pattern is not unique and its choice strongly affects the total harmonic distortions (THDs) of the side-1 and side-2 waveforms.

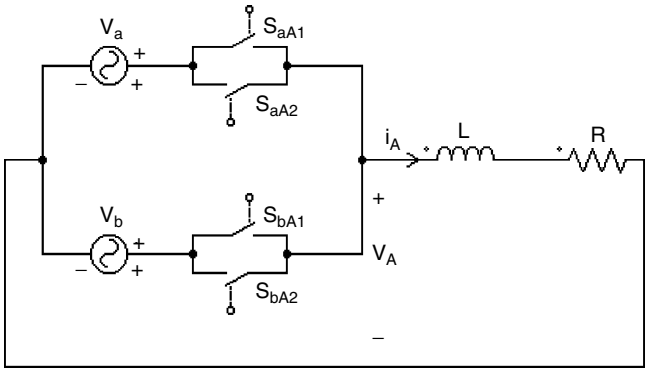

Figure 15.11 Two bidirectional switches S_{aA} and S_{bA} commutating the phase A current [11].

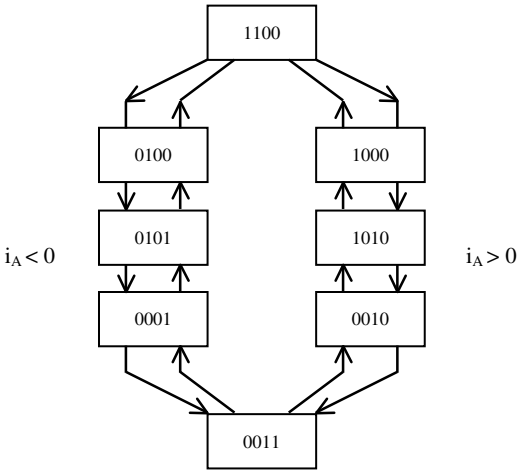

Figure 15.12 Switching sequence diagram for safe operation of S_{aA} and S_{bA} [11].

Furthermore, in order to obtain high-quality waveforms, a high switching frequency has to be adopted. In order to avoid a dead-time or an overlap between the on-states of the bidirectional switches connecting two input phases to one output phase while commutating an inductive load current, a multistep switching strategy is used. Figure 15.11 shows the two bidirectional switches S_{aA} and S_{bA} connecting the input phases a and b to the output phase A. Figure 15.12 shows a special four-step switching sequence proposed in Reference 11 for the control of the two-quadrant switch elements of the bidirectional switches shown in Figure 15.11, to protect the matrix converter switches against hazardous conditions. The 4-bit switch status code shown in Figure 15.12 represents the positions of the switches S_{aA1}, S_{aA2}, S_{bA1}, and S_{bA2}, respectively, where 1 stands for on position and 0 stands for off position. As shown in Figure 15.12, the two-quadrant switch elements of each bidirectional switch are controlled individually to avoid any dead-time or overlap between the on-states of the bidirectional switches. As the switching frequencies are high, the implementation of the four-step switching strategy of Figure 15.12 requires very fast controller and switches.

The main advantages of matrix converters lie in their compact design (due to the elimination of the DC-link reactive element), the possibility of simultaneous power factor correction at the input and vector control at the output, and the high-quality waveforms on both sides. The main disadvantages of matrix converters are: high switching losses, complexity of control, lack of energy storage leading to practically zero ride-through capacity, and direct transfer of harmonic distortion and imbalance in the side-1 voltage and side-2 current to the side-2 voltage and side-1 current.

Based on Figure 15.9, the voltage and current transformations in an FCC are given by

$$\begin{bmatrix} v_{2A} \\ v_{2B} \\ v_{2C} \end{bmatrix} = [S] \begin{bmatrix} v_{1a} \\ v_{1b} \\ v_{1c} \end{bmatrix} \tag{15.1}$$

and

$$\begin{bmatrix} i_{1a} \\ i_{1b} \\ i_{1c} \end{bmatrix} = [S]^T \begin{bmatrix} i_{2A} \\ i_{2B} \\ i_{2C} \end{bmatrix}, \tag{15.2}$$

where $[S]$ is the existence matrix composed of time-varying entries that assume binary values of 1 or 0 for on or off state of the nine bidirectional switches, respectively. As far as the fundamental components of the voltages and currents on both sides are concerned, the matrix $[S]$ can be replaced by the transformation matrix $[H]$ whose elements are the local averages of the corresponding elements of the $[S]$ matrix. The structure of a typical $[H]$ matrix is as follows [12]:

$$H = \begin{bmatrix} h_{11} & h_{12} & h_{13} \\ h_{21} & h_{22} & h_{23} \\ h_{31} & h_{32} & h_{33} \end{bmatrix} = 1/3 \begin{bmatrix} 1 & 1 & 1 \\ 1 & 1 & 1 \\ 1 & 1 & 1 \end{bmatrix} \tag{15.3}$$

$$+ M_1 \begin{bmatrix} \cos[(\omega_1+\omega_2)t+\gamma] & \cos[(\omega_1+\omega_2)t-120^\circ+\gamma] & \cos[(\omega_1+\omega_2)t+120^\circ+\gamma] \\ \cos[(\omega_1+\omega_2)t-120^\circ+\gamma] & \cos[(\omega_1+\omega_2)t+120^\circ+\gamma] & \cos[(\omega_1+\omega_2)t+\gamma] \\ \cos[(\omega_1+\omega_2)t+120^\circ+\gamma] & \cos[(\omega_1+\omega_2)t+\gamma] & \cos[(\omega_1+\omega_2)t-120^\circ+\gamma] \end{bmatrix}.$$

$$+ M_2 \begin{bmatrix} \cos[(\omega_1-\omega_2)t-\gamma] & \cos[(\omega_1-\omega_2)t+120^\circ-\gamma] & \cos[(\omega_1-\omega_2)t-120^\circ-\gamma] \\ \cos[(\omega_1-\omega_2)t-120^\circ-\gamma] & \cos[(\omega_1-\omega_2)t-\gamma] & \cos[(\omega_1-\omega_2)t+120^\circ-\gamma] \\ \cos[(\omega_1-\omega_2)t+120^\circ-\gamma] & \cos[(\omega_1-\omega_2)t-120^\circ-\gamma] & \cos[(\omega_1-\omega_2)t-\gamma] \end{bmatrix}$$

Note that for the elements of $[H]$ matrix to represent the local averages of the elements of $[S]$ matrix, the following existence condition must be satisfied [13]:

$$0 \le h_{ij} \le 1 \quad \text{for} \quad i = 1, 2, 3 \quad \text{and} \quad j = 1, 2, 3 \tag{15.4}$$

Also, for one and only one of the switches connecting the three phases on side-1 to each phase on side-2 to be on at any instant, the following condition must be met [13]:

$$\sum_{j=1}^{3} h_{ij} = 1 \quad \text{for} \quad i = 1, 2, 3 \tag{15.5}$$

Assuming that

$$\begin{bmatrix} v_{1a} \\ v_{1b} \\ v_{1c} \end{bmatrix} = \begin{bmatrix} V_{1m} \cos \omega_1 t \\ V_{1m} \cos(\omega_1 t - 120^\circ) \\ V_{1m} \cos(\omega_1 t + 120^\circ) \end{bmatrix}, \tag{15.6}$$

one can find

$$\begin{bmatrix} v_{2A} \\ v_{2B} \\ v_{2C} \end{bmatrix} = \begin{bmatrix} H \end{bmatrix} \begin{bmatrix} v_{1a} \\ v_{1b} \\ v_{1c} \end{bmatrix} = 3/2\,(M_1 + M_2) V_{1m} \begin{bmatrix} \cos(\omega_2 t + \gamma) \\ \cos(\omega_1 t - 120^\circ + \gamma) \\ \cos(\omega_1 t + 120^\circ + \gamma) \end{bmatrix} \tag{15.7}$$

The voltage gain of the matrix converter can therefore be expressed as

$$G_v = \frac{V_{2m}}{V_{1m}} = 3/2\,(M_1 + M_2) \tag{15.8}$$

Also, assuming that

$$\begin{bmatrix} i_{2A} \\ i_{2B} \\ i_{2C} \end{bmatrix} = I_{2m} \begin{bmatrix} \cos(\omega_2 t + \gamma + \phi_2) \\ \cos(\omega_2 t - 120^\circ + \gamma + \phi_2) \\ \cos(\omega_2 t + 120^\circ + \gamma + \phi_2) \end{bmatrix}, \tag{15.9}$$

one can find

$$\begin{bmatrix} i_{1a} \\ i_{1b} \\ i_{1c} \end{bmatrix} = \begin{bmatrix} H \end{bmatrix}^T \begin{bmatrix} i_{2A} \\ i_{2B} \\ i_{2C} \end{bmatrix} = I_{1m} \begin{bmatrix} \cos(\omega_1 t + \phi_1) \\ \cos(\omega_1 t + \phi_1 - 120^\circ) \\ \cos(\omega_1 t + \phi_1 + 120^\circ) \end{bmatrix}, \tag{15.10}$$

where

$$I_{1m} = 3/2\, I_{2m} \sqrt{M_1^2 + M_2^2 + 2 M_1 M_2 \cos 2\phi_2} \tag{15.11}$$

and

$$\phi_1 = -\tan^{-1}\left(\frac{M_1 - M_2}{M_1 + M_2} \tan \phi_2 \right). \tag{15.12}$$

From Equation 15.8 and Equation 15.12, one can find the values for M_1 and M_2 that satisfy the specifications on the desired voltage gain and side-1 displacement angle as follows:

$$M_1 = 1/3\, G_v \left(1 - \frac{\tan \phi_1}{\tan \phi_2} \right) \tag{15.13}$$

and

$$M_2 = 1/3\, G_v \left(1 + \frac{\tan \phi_1}{\tan \phi_2} \right). \tag{15.14}$$

As seen, the conventional 9-bidirectional-switch matrix converter has 3 levers of control; i.e., M_1, M_2, and γ. M_1 and M_2 are used to control the magnitude of the side-2 voltage and the side-1 displacement power factor, whereas γ is used to control the phase angle of the side-2 voltage. All together, the three levers of control are able to control the active power flow as well as the side-1 and side-2 reactive powers independent of each other.

Common control techniques applied to conventional matrix converter topology include scalar control methods that are based on the instantaneous values of the input voltages and transfer function analysis [12,14,15], and space vector modulation [16]. Even though based on Equation 15.8, the maximum attainable voltage gain of the matrix converter, within the limits imposed by Equation 15.4, is 1, due to physical constraints and regardless of the switching strategy used, the highest gain that can be achieved in practice is 0.866 [10]. This gain can be improved to 1.05 using space vector modulation involving overmodulation at the price of higher harmonic contents and higher filter requirements [10]. The principle of matrix conversion has been also used to realize frequency changers made up of unidirectional switches only [17–19]. In these frequency changers, the inherent switching problems of conventional matrix converter is avoided.

As far as the specific application of hybrid electric vehicle is concerned, matrix converters provide input power factor correction, output vector control, bidirectional power flow, compact design (i.e., high-power density), high-quality waveforms, and unrestricted frequency conversion. The fact that matrix converters, as well as NCCs, lack ride-through capacity is not a serious issue in the specific application of parallel HEV designs, as the ICE would be able to supply the power directly to the wheels in case of temporary interruption in the electric power. The fact that there is no place for the integration of an energy storage battery in the matrix converter and NCC system, without an additional converter, remains a disadvantage. However, if a flywheel is used as the energy storage device, this problem can be solved [20]. Figure 15.13 and Figure 15.14 show two possible serial and parallel HEV designs based on matrix converter and NCC.

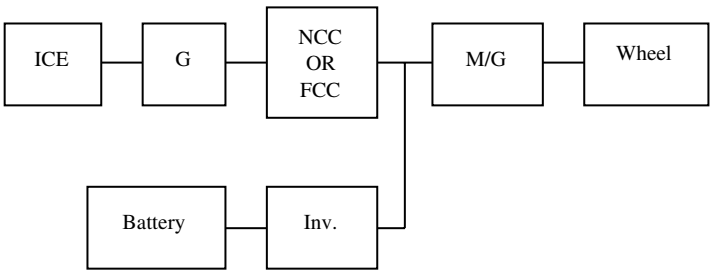

Figure 15.13 Potential serial HEV design using NCC or FCC (matrix converter).

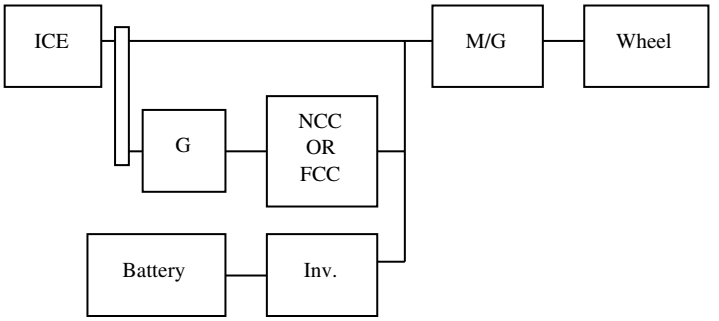

Figure 15.14 Potential parallel HEV design using NCC or FCC (matrix converter).

Note that in all the HEV configurations based on AC/AC converters, the internal combustion engine can be replaced or assisted by a flywheel that stores mechanical energy and can be recharged through an external circuit, ICE, battery, or wheels (during regenerative breaking) [20]. Also, a hydrogen-fueled fuel cell, as a source of electrical energy, can be incorporated in the system.

15.3 SUMMARY

With the evolution of more electric vehicles, the role of power electronics as a power conditioning tool becomes more vital. Hybrid electric vehicles, due to their high efficiency, flexibility, and reliability, are receiving more attention compared with totally electric vehicles. This chapter introduces the structures, principles of operation, advantages, and disadvantages of the three main types of AC/AC converters, i.e., rectifier-inverter pair, naturally commutated cycloconverter, and forced-commutated cycloconverter (or matrix converter), and their potential roles in the automotive industry, especially in hybrid electric vehicles.

The factors affecting the choice of a certain AC/AC converter topology are the cost, weight, size, waveform quality, efficiency, robustness, reliability, filter requirements, ride-through capability, immunity to harmonics distortion and imbalance, reactive power requirements, control complexity, restriction of the input/output frequency ratio, and input power factor correction capability. Even though the rectifier-inverter pair and NCC topologies are well-established and accepted by the industry, there is a high potential for other types of AC/AC converters.

Matrix converters with unrestricted frequency conversion ability, compact design, and input power factor correction capability seem to be a good candidate for AC/AC conversion in hybrid electric vehicles. The lack of ride-through capability will not be a serious issue in the hybrid electric vehicle of parallel design, where a temporary interruption in the electric power can be compensated by the internal combustion engine under a proper control regime. However, the success of matrix converters will depend on the availability of monolithic bidirectional switches. Soft-switched high-frequency converters are another eligible candidate for AC/AC converters in the automotive industry due to their high efficiency and high-power density. However, they have to prove to be cost-effective and reliable before winning against more established competitors.

REFERENCES

[1] P. Bowler. The Application of a Cycloconverter to the Control of Induction Motors. *Proceedings of IEE Conference on Power Applications of Controllable Semiconductor Devices*, No. 17, pp. 137–145, 1965.

[2] L. Malesani, L. Rossetto, P. Tenti, P. Tomasin. AC/DC/AC PWM Converter with Reduced Energy Storage in the DC Link. *IEEE Transactions in Industry Applications*, Vol. 31, No. 2, pp. 287–292, 1995.

[3] S. Bhowmik, R. Spee. A Guide to the Application-Oriented Selection of AC/AC Converter Topologies. *IEEE Transactions on Power Electronics*, Vol. 8, No. 2, pp. 156–163, 1993.

[4] L.J. Jacovides, M.F. Matouka, D.W. Shimer. A Cycloconverter-Synchronous Motor Drive for Traction Applications. *IEEE Transactions on Industry Applications*, pp. 549–561, 1980.

[5] L.J. Lawson. The Practical Cycloconverter. *IEEE Transactions on Industry and General Applications*, Vol. IGA-4, No. 2, pp. 141–144, 1968.

[6] J. Vithayathil. *Power Electronics: Principles and Applications.* New York: McGraw-Hill, pp. 519–527, 1995.

[7] G.K. Dubey. *Power Semiconductor Controlled Drives,* 1st Ed. Englewood Cliffs, NJ: Prentice-Hall, pp. 345–349, 1989.

[8] L. Gyugyi, B.R. Pelly. *Static Power Frequency Changers: Theory, Performance, and Application.* New York: John Wiley & Sons, 1976.

[9] S. Bernet, T. Matsuo, T.A. Lipo. A Matrix Converter Using Reverse Blocking NPT-IGBTs and Optimized Pulse Patterns. *Proceedings of IEEE Power Electronics Specialists Conference (PESC),* Baveno, Italy, pp. 107–112, 1996.

[10] M.H. Rashid. *Power Electronics: Circuits, Devices, and Applications,* 3rd Ed. Englewood Cliffs, NJ: Pearson Prentice-Hall, pp. 536–537, 2003.

[11] N. Burany. Safe Control of 4-Quadrant Switches. *Proceedings of IEEE Industry Applications Society Annual Meeting,* San Diego, CA, pp. 1190–1194, 1989.

[12] M. Venturini, A. Alesina. The Generalized Transformer: A New Bidirectional Sinusoidal Waveform Frequency Changer with Continuously Adjustable Input Power Factor. *Proceedings of IEEE Power Electronics Specialists Conference*, pp. 242–252, 1980.

[13] D.G. Holmes. A Unified Modulation Algorithm for Voltage and Current Source Inverters Based on AC-AC Matrix Converter Theory. *IEEE Transactions on Industry Applications*, Vol. 28, No. 1, pp. 31–40, 1992.

[14] G. Roy, G.E. April. Direct Frequency Changer Operation Under a New Scalar Control Algorithm. *IEEE Transactions on Power Electronics*, Vol. 6, No. 1, pp. 100–107, 1991.

[15] A. Ishiguro, T. Furuhashi, S. Okuma. A Novel Control Method for Forced-Commutated Cycloconverters using Instantaneous Values of Input Line-to-Line Voltages. *IEEE Transactions on Industrial Electronics*, Vol. 38, No. 3, pp. 166–172, 1991.

[16] L. Huber, D. Borojevic. Space Vector Modulated Three-Phase to Three-Phase Matrix Converter with Input Power Factor Correction. *IEEE Transactions on Industry Applications*, Vol. 31, pp. 1234–1246, 1995.

[17] M. Kazerani, B.T. Ooi. Feasibility of both Vector Control and Displacement Factor Correction by Voltage Source Type AC-AC Matrix Converter. *IEEE Transactions on Industrial Electronics*, Vol. 42, No. 5, pp. 524–530, 1995.

[18] M. Kazerani. A Direct AC/AC Converter Based on Current-Source Converter Modules. *IEEE Transactions on Power Electronics*, Vol. 18, No. 5, pp. 1168–1175, 2003.

[19] S. Kim, S.K. Sul, T.A. Lipo. AC to AC Power Conversion Based on Matrix Converter Topology with Unidirectional Switches. *Proceedings of IEEE Applied Power Electronics Conference*, Anaheim, CA, pp. 301–307, 1998.

[20] G.J. Hoolboom, B. Szabados. Nonpolluting Automobiles. *IEEE Transactions on Vehicular Technology*, Vol. 43, No. 4, pp. 1136–1144, November 1994.